HHS Public Access

Author manuscript

J Urol. Author manuscript; available in PMC 2015 April 28.

Published in final edited form as:

J Urol. 2014 May ; 191(5): 1439–1445. doi:10.1016/j.juro.2013.10.041.

A Prospective Pilot Study of ^{89}Zr-J591/Prostate Specific Membrane Antigen Positron Emission Tomography in Men with Localized Prostate Cancer Undergoing Radical Prostatectomy

Joseph R. Osborne, **David A. Green**, **Daniel E. Spratt**, **Serge Lyashchenko**, **Shoaib B. Fareedy**, **Brian D. Robinson**, **Bradley J. Beattie**, **Manu Jain**, **Jason S. Lewis**, **Paul Christos**, **Steven M. Larson**, **Neil H. Bander***, and **Douglas S. Scherr**†

Molecular Imaging and Therapy Service (JRO, SBF, SML) and Radiochemistry and Imaging Sciences Service (SL, JSL), Department of Radiology, Department of Radiation Oncology (DES) and Department of Medical Physics (BJB), Memorial Sloan-Kettering Cancer Center and Department of Urology (DAG, BDR, MJ, NHB, DSS), Division of Biostatistics and Epidemiology, Department of Public Health (PC) and Department of Pathology (BDR), Weill Medical College of Cornell University, New York, New York

Abstract

Purpose—In this pilot study we explored the feasibility of ^{89}Zr labeled J591 monoclonal antibody positron emission tomography of localized prostate cancer.

Materials and Methods—Before scheduled radical prostatectomy 11 patients were injected intravenously with ^{89}Zr-J591, followed 6 days later by whole body positron emission tomography. Patients underwent surgery the day after imaging. Specimens were imaged by ex vivo micro positron emission tomography and a custom 3 Tesla magnetic resonance scanner coil. Positron emission tomography images and histopathology were correlated.

Results—Median patient age was 61 years (range 47 to 68), median prostate specific antigen was 5.2 ng/ml (range 3.5 to 12.0) and median biopsy Gleason score of the 11 index lesions was 7 (range 7 to 9). On histopathology 22 lesions were identified. Median lesion size was 5.5 mm (range 2 to 21) and median Gleason score after radical prostatectomy was 7 (range 6 to 9). Eight of 11 index lesions (72.7%) were identified by in vivo positron emission tomography. Lesion identification improved with increasing lesion size for in vivo and ex vivo positron emission tomography (each $p < 0.0001$), and increasing Gleason score ($p = 0.14$ and 0.01, respectively). Standardized uptake values appeared to correlate with increased Gleason score but not significantly ($p = 0.19$).

Conclusions—To our knowledge this is the first report of ^{89}Zr-J591/prostate specific membrane antigen positron emission tomography in localized prostate cancer cases. In this setting ^{89}Zr-J591 bound to tumor foci in situ and positron emission tomography identified primarily Gleason score 7

†Correspondence: Department of Urology, Weill Medical College of Cornell University, Starr 900, 525 East 68th St., Box 94, New York, New York 10065 (telephone: 212-746-5788; FAX: 212-746-8068; dss2001@med.cornell.edu).

*Financial interest and/or other relationship with BZL Biologics.

Study received Weill Cornell Medical College institutional review board approval.

or greater and larger tumors, likely corresponding to clinically significant disease warranting definitive therapy. A future, larger clinical validation trial is planned to better define the usefulness of ^{89}Zr-J591 positron emission tomography for localized prostate cancer.

Keywords

prostatic neoplasms; positron-emission tomography; glutamate carboxypeptidase II; human; zirconium; J591 monoclonal antibody

Imaging is critical for accurate PCa diagnosis and staging. For the last 30 years localized PCa imaging has largely relied on TRUS. An estimated 37% to 50% of PCas are isoechoic to the normal peripheral zone and, thus, not visible on TRUS.[1] Furthermore, in a series of more than 33,000 prostate biopsies only 44.6% of men were found to have PCa, highlighting the inadequacy of the essentially blind TRUS guided biopsy.[2]

In the last decade endorectal MRI and more recently mpMRI have increasingly been used to stage localized PCa. While mpMRI has improved the accuracy of staging and biopsy sensitivity,[3] the AJCC (American Joint Committee on Cancer) does not recommend incorporating MRI findings to determine clinical T stage,[4] nor has the National Comprehensive Cancer Network routinely recommended MRI for staging. These recommendations are driven by the modest sensitivity and specificity of mpMRI (76% and 82%, respectively),[5] and by conflicting data on its prognostic value before treatment.[6]

Unlike for many other solid tumors FDG PET has limited usefulness for localized PCa.[7] Additional PET tracers tested in men have shown modest success. ^{11}C-choline and ^{18}F-choline have efficacy primarily in the biochemically recurrent and meta-static settings rather than for localized disease.[7–10] ^{11}C-acetate aids in identifying lymph node metastases with modest sensitivity and specificity.[11] An imaging biomarker annotating clinically significant PCa in localized disease cases would have a dramatic impact on diagnosis, staging, treatment planning and response monitoring.

PSMA, a transmembrane cell protein, is heterogeneously expressed by normal prostate luminal epithelial cells and highly up-regulated in PCa.[12] PSMA is expressed by more than 90% to 95% of PCas with increased expression in higher grade, metastatic and castrate resistant disease.[13,14] Several studies showed a correlation between the expression level and the rate/incidence of biochemical recurrence as well as overall survival.[13,15,16]

J591, a humanized monoclonal antibody that binds specifically to the PSMA extracellular domain, was developed and extensively studied in vivo in meta-static castration resistant PCa.[17–21] The demonstrated success of J591 as an imaging and therapeutic targeting agent in the metastatic setting[22] along with more recent first in human ^{89}Zr-J591 data in patients with metastatic, castrate resistant PCa make this a leading candidate as a molecular imaging biomarker. After the development of a safe chelating agent (DFO), preclinical studies demonstrating efficacy and dosimetry, and following Food and Drug Administration guidelines for biomarker development we report what is to our knowledge the first human data on ^{89}Zr-J591 PET tracer in localized PCa and its preliminary assessment in the first 11 patients.

MATERIALS AND METHODS

Patient Selection and Data Collection

The Weill Cornell Medical College institutional review board approved this prospective pilot study. Patients at the Department of Urology, Weill Cornell Medical College/New York-Presbyterian Hospital were evaluated for study participation after the decision was made to pursue RP. All men were required to have a biopsy Gleason score of 7 or greater and localized PCa based on pretreatment staging evaluation with TRUS guided prostate biopsy, ^{99m}Tc bone scan and endorectal 3 Tesla MRI. Study exclusion criteria were a history of hormonal therapy, radiotherapy to the prostate or metastatic disease.

Antibody Preparation and Administration

^{89}Zr-DFO-J591 was produced and administered under Investigational New Drug No. 115521. ^{89}Zr was produced in a cyclotron using the ^{89}Y(p,n)^{89}Zr transmutation reaction and isolated in high radionuclide and radiochemical purity (greater than 99.99%) as ^{89}Zr-oxalate using a solid phase hydroxamate resin. The effective specific activity of ^{89}Zr was found to be in the range of 5.28 to 13.43 mCi/μg (470 to 1,195 Ci/mmol) Zr.

The antibody was conjugated to DFO at room temperature. In vitro stability measurements confirmed that ^{89}Zr-DFO is stable in human serum for more than 7 days.

Patients were premedicated with intravenous diphenhydramine (25 mg) and oral acetaminophen (650 mg). They were first injected with 20 mg of unlabeled J591 antibody at a rate of 5 mg or less of antibody per minute. Two minutes after completion they received a second injection of ^{89}Zr-J591 (5 mCi/2 mg of J591). They were monitored for 4 hours after injection.

In Vivo ^{89}Zr-J591 PET

Imaging was done 5 to 7 days after injection. Whole body (^{89}Zr-J591) PET/CT was acquired. The specifications were CT at 80 kV and 20 mA, and PET at 3 minutes per bed scanned from the top of the skull through the thighs for a total scan time of 40 to 50 minutes to determine whole body distribution. This was immediately followed by limited 30-minute PET/CT of the pelvis.

Ex Vivo PET

Patients underwent RP with bilateral pelvic lymphadenectomy the day after PET. Immediately after surgical excision RP specimens were brought to our small animal imaging facility on site for ex vivo imaging on an Inveon™ microPET/CT preclinical scanner. List mode data were acquired for 30 minutes using an energy window of 350 to 650 keV and a coincidence timing window of 3.432 nanoseconds. Data were sorted into 3-dimensional histograms using a span of 3 and a ring difference of 79. Images were reconstructed with the 3-dimensional maximum a posteriori algorithm to a 0.097 × 0.097 mm pixel size and 0.796 mm slice thickness.

Histology Evaluation

Prostate specimen preparation—After ex vivo imaging the prostate was transported immediately to surgical pathology for routine gross and microscopic evaluation. Briefly, the prostate was weighed, oriented and inked according to institutional protocol. The apical (distal urethral) and basal (proximal urethral) margins were shaved, perpendicularly sectioned and submitted. The remaining prostate was serially sectioned into 5 mm slices starting from the apex with sections made perpendicular to the urethra. These serial sections were then further quartered to fit into standard processing cassettes. All prostates were entirely submitted for histological evaluation. Tissues were fixed in 10% neutral buffered formalin, processed and paraffin embedded. Sections (5 mm) were stained with hematoxylin and eosin for microscopic review.

Tumor mapping—All tumor foci on hematoxylin and eosin stained slides were marked by study pathologists (BDR, MJ) and assigned a Gleason score. A map was drawn for each prostatectomy specimen with tumor foci marked according to location (anterior/posterior, left/right) for each serial 5 mm slice (apex to base).

Immunohistochemistry for PSMA—The dominant and secondary tumor nodules were stained for PSMA to confirm PSMA expression. Staining was performed on the BOND™ III Autostainer using reagents supplied by the manufacturer except when otherwise specified. Sections (5 mm) were deparaffinized and endogenous peroxidase was inactivated, followed by heat induced epitope retrieval-1 (Leica Microsystems, Wetzlar, Germany) according to manufacturer instructions. Primary mouse monoclonal antibody for PSMA (clone 3E6, Dako®) was detected using the Refine Detection Kit (Leica Microsystems). As the chromogen, we used 3,3′-diaminobenzidine with hematoxylin used for counterstaining.

Radiological-Pathological Correlation and SUV Calculation

Our study committee determined the presence or absence of signal at the appropriate anatomical location that corresponded to the lesion location on histopathology. Thus, each index and secondary lesion noted on histopathology was determined to be visible or not visible on in vivo and ex vivo PET. Reviewers were not blinded to pathology findings since this was a phase 0 pilot study to assess the feasibility of targeting ^{89}Zr-J591 antibody in the prostate gland. Also, SUV was measured for each lesion that was visible on ex vivo PET.

Statistical Analysis

Descriptive statistics were calculated to characterize the study cohort. The Wilcoxon rank sum test was used to compare lesion size/Gleason score between lesions that were and were not identified by 1) ex vivo PET and 2) in vivo PET. The Spearman rank correlation coefficient was used to correlate SUV with Gleason score. All p values are 2-sided with statistical significance evaluated at the 0.05 α level. P values should be considered for hypothesis generating purposes since the goal of this pilot study was to preliminarily evaluate the feasibility of ^{89}Zr-J591 for localized PCa. All analysis was done with SPSS®, version 21.0.

RESULTS

A total of 11 patients completed the protocol and no injection or imaging related adverse event was noted. Table 1 lists the basic clinicopathological features of the cohort. Median age was 61 years (range 47 to 68 years), median PSA was 5.2 ng/ml (range 3.5 to 12.0) and median biopsy Gleason score of the 11 index lesions was 7 (range 7 to 9). After surgery 22 lesions were identified on histopathology. Median lesion size was 5.5 mm (range 2 to 21) and median post-RP Gleason score was 7 (range 6 to 9). Table 2 lists the pathological features of these lesions. Notably, surgical margins and lymph node involvement were negative on histopathology in all patients. In addition, no lymph nodes were PET avid.

A total of 22 PCa lesions were identified, including 11 considered index lesions. Eight of 11 index lesions (72.7%) were identified on in vivo PET. All index lesions were visualized by ex vivo PET. Four of 11 secondary nodules (36.4%) were visualized on ex vivo PET. Of the 7 secondary nodules not seen on ex vivo PET 6 were Gleason 3 + 3 = 6 cancer and 1 was a 2 mm focus of Gleason 4 + 5 = 9. Lesion identification improved with increasing lesion size for in vivo PET (detected vs undetected 15 vs 4 mm, $p < 0.0001$) and ex vivo PET (detected vs undetected 12 vs 3 mm, $p < 0.0001$). Lesion identification also improved with increasing Gleason score for in vivo PET. The median Gleason score of detected vs undetected lesions was 7 vs 6 ($p = 0.14$) and for ex vivo PET it was 7 vs 6 ($p = 0.01$, fig. 1, A). Increases in ex vivo PET SUV also correlated with increases in Gleason score (Spearman rank correlation coefficient 0.36, $p = 0.19$, fig. 1, B). Immunohistochemical staining confirmed that all index lesions and secondary nodules expressed PSMA.

Figure 2 shows a large Gleason 9 lesion with low signal intensity and restricted diffusion on mpMRI. In vivo and ex vivo PET revealed a highly J591 avid lesion, a finding that corresponded anatomically to MRI and histopathology results. Figure 3 shows a Gleason 7 cancer with low suspicion on mpMRI but significant tracer uptake on PET. Figure 4 shows multifocal Gleason 3 + 4 and 4 + 3 PCa that was suspicious on mpMRI. Each lesion was J591 avid.

On ex vivo PET 1 patient had prominent uptake in a nodule, which proved to be benign prostatic hyperplasia (fig. 5). The SUV of the benign nodule was 5 and the Gleason 8 focus was 3. Upon histological review a prominent inflammatory reaction was noted in this avid, benign prostatic hyperplasia nodule.

DISCUSSION

This pilot study confirms binding of ^{89}Zr-J591 to PCa foci in vivo. The protocol included ex vivo specimen PET-MRI to allow us to directly correlate J591 binding with MRI and pathological findings. In this relatively small feasibility study in vivo J591 PET detected 8 of 11 index lesions while ex vivo specimen PET identified all 11 index lesions and 21 of 22 lesions that were Gleason 7 or greater. Combined with preliminary data correlating the detection of high grade lesions with increased SUV these findings suggest that noninvasive J591 PET may provide biologically and clinically relevant information.

PSMA, the antigen targeted by J591, is highly up-regulated in PCa. It also is expressed by some nonmalignant prostate epithelium. However, normal PSMA membrane expression is on the luminal aspect of the gland and, thus, it is sequestered from exposure to circulating antibody. This allows for a dramatic inherent contrast that is ideal for imaging. This phenomenon was also noted for PSA with a million-fold ratio of PSA in the glandular lumen relative to plasma.

Despite this preferential effect of normal to malignant tissue we noted false-positive detection using ^{89}Zr-J591. In 1 patient an area in the prostate without histological evidence of tumor showed increased tracer uptake. Histopathology correlation revealed a benign hot spot in the transition zone with prominent inflammatory infiltrate. As in other solid tumor imaging using FDG PET, anatomical imaging modalities such as mpMRI would likely mitigate many of these false-positive findings.

These preliminary results suggest several potential future applications of J591 PET in localized PCa. 1) Molecular imaging with J591 PET may have a role in treating men on active surveillance programs. By identifying lesion site(s) for biopsy and with SUV correlation with Gleason score it may be possible to improve patient selection. In addition, serial imaging may allow the identification of new lesions and/or a change in Gleason grade signaled by increased SUV. 2) Molecular imaging with ^{89}Zr-J591 PET may have a role in image guided focal therapy. Our early data show that ^{89}Zr-J591 PET enables the identification of some index lesions that are not detected by mpMRI, suggesting that combining these modalities may improve accurate detection of clinically significant disease to define a patient population appropriate for focal therapy. 3) As index lesions are treated, ^{89}Zr-J591 PET may provide an early metric of successful ablation. One would anticipate the loss of ^{89}Zr-J591 PET signal in case of successful ablation and/or reemergence of a hot lesion in case of a new focus or recurrent lesion.

One of the greatest posttreatment challenges is monitoring for response/recurrence. Biopsy of post-radiotherapy glands is particularly difficult to interpret and often shows adenocarcinoma with a treatment effect but there is no clinical means of assessing the biological activity of these lesions.[23] While to our knowledge it remains to be proven, PSMA based imaging may provide biological insights into these tumors. Post-radiotherapy ^{89}Zr-J591 imaging is currently under way in pre-clinical studies and it will be incorporated into a high risk phase I/II trial in the near future.

Beyond the benefit of identifying aggressive foci in the prostate ^{89}Zr-J591 PET may provide clinical value in men with clinically localized but high risk disease to detect early metastatic lesions. Men with extraprostatic extension, Gleason 8 or greater, or pretreatment PSA 20 ng/ml or greater are at high risk for lymph node and potentially distant micrometastatic disease. Data on our metastatic PCa cohort in which ^{89}Zr-J591 PET was performed indicate significantly improved sensitivity over bone scan, CT, MRI and FDG PET. Low volume meta-static disease that is undetectable on standard imaging has been visualized and biopsy confirmed on ^{89}Zr-J591 PET.[24] As our imaging cohort expands and our data mature, this will be an area on which to focus clinical attention.

A limitation of current ^{89}Zr-J591 PET is the 5 to 7-day waiting period between injection and imaging due to the long clearance time of intact antibodies. To overcome this a J591 minibody, that is an antibody fragment of approximately 80 kDa that maintains the divalent binding property against PSMA, was engineered and developed. Due to its smaller size and absent FcRY binding site the minibody has faster clearance from circulation as well as potentially enhanced penetration when targeting tumor tissue. Clinical studies of this agent are planned.

CONCLUSIONS

In vivo ^{89}Zr-J591 PET can identify discrete intraprostatic tumor foci and in our cohort it visualized most index lesions. Also, high grade tumors are generally better visualized with this novel imaging agent. There is a relationship between SUV on ^{89}Zr-J591 PET of tumor foci and tumor aggressiveness, as defined by Gleason score. Preliminary data from this pilot study provide a basis on which to investigate the various roles of ^{89}Zr-J591 PET in PCa diagnosis, management and treatment. Among others, such areas of future investigation should include incorporation into active surveillance algorithms, fusion imaging biopsy platforms, image guidance for focal therapy and monitoring the therapeutic response.

Acknowledgments

Supported by Center to Reduce Cancer Health Disparity Grant R21 CA153177-03 (JRO, SBF, BJB), the Starr Consortium, Ludwig Center for Targeted Radioimmunotherapy and Diagnosis, Geoffrey Beane Cancer Consortia, and Radiochemistry and Molecular Imaging Probe Core (JSL, SML and SL), David H. Koch Foundation, Robert Dow Foundation, and Frederick J. and Theresa Dow Wallace Fund of New York Community Trust (DAG, DSS, NHB), Clinical Translational Science Center Grant UL1-TR000457-06 (PC) and the James P. McCarron Foundation.

Kofi Deh, and Drs. Jonathan Dyke and Bin He assisted with instrumentation. The J591 minibody was developed at ImaginAb, Inglewood, California.

Abbreviations and Acronyms

CT	computerized tomography
DFO	deferoxamine
FDG	fluorodeoxyglucose
mpMRI	multiparametric
MRI MRI	magnetic resonance imaging
PCa	prostate cancer
PET	positron emission tomography
PSA	prostate specific antigen
PSMA	prostate specific membrane antigen
RP	radical prostatectomy
SUV	standardized uptake value

TRUS transrectal ultrasound

References

1. Vo T, Rifkin MD, Peters TL. Should ultrasound criteria of the prostate be redefined to better evaluate when and where to biopsy. Ultrasound Q. 2001; 17:171. [PubMed: 12973073]
2. Nam RK, Saskin R, Lee Y, et al. Increasing hospital admission rates for urological complications after transrectal ultrasound guided prostate biopsy. J Urol, suppl. 2013; 189:S12.
3. Delongchamps NB, Rouanne M, Flam T, et al. Multiparametric magnetic resonance imaging for the detection and localization of prostate cancer: combination of T2-weighted, dynamic contrast-enhanced and diffusion-weighted imaging. BJU Int. 2011; 107:1411. [PubMed: 21044250]
4. Edge, S.; Byrd, DR.; Compton, CC., et al. AJCC Staging Manual. 7. New York: Springer; 2010.
5. Wu LM, Xu JR, Ye YQ, et al. The clinical value of diffusion-weighted imaging in combination with T2-weighted imaging in diagnosing prostate carcinoma: a systematic review and meta-analysis. AJR Am J Roentgenol. 2012; 199:103. [PubMed: 22733900]
6. Mowatt G, Scotland G, Boachie C, et al. The diagnostic accuracy and cost-effectiveness of magnetic resonance spectroscopy and enhanced magnetic resonance imaging techniques in aiding the localisation of prostate abnormalities for biopsy: a systematic review and economic evaluation. Health Technol Assess. 2013; 17:1. [PubMed: 23870108]
7. Fox JJ, Schoder H, Larson SM. Molecular imaging of prostate cancer. Curr Opin Urol. 2012; 22:320. [PubMed: 22617062]
8. Souvatzoglou M, Weirich G, Schwarzenboeck S, et al. The sensitivity of [11C]choline PET/CT to localize prostate cancer depends on the tumor configuration. Clin Cancer Res. 2011; 17:3751. [PubMed: 21493868]
9. Bauman G, Belhocine T, Kovacs M, et al. 18F-fluorocholine for prostate cancer imaging: a systematic review of the literature. Prostate Cancer Prostatic Dis. 2012; 15:45. [PubMed: 21844889]
10. Krause BJ, Souvatzoglou M, Tuncel M, et al. The detection rate of [11C]choline-PET/CT depends on the serum PSA-value in patients with biochemical recurrence of prostate cancer. Eur J Nucl Med Mol Imaging. 2008; 35:18. [PubMed: 17891394]
11. Haseebuddin M, Dehdashti F, Siegel BA, et al. 11C-acetate PET/CT before radical prostatectomy: nodal staging and treatment failure prediction. J Nucl Med. 2013; 54:699. [PubMed: 23471311]
12. Bander NH. Technology insight: monoclonal antibody imaging of prostate cancer. Nat Clin Pract Urol. 2006; 3:216. [PubMed: 16607370]
13. Perner S, Hofer MD, Kim R, et al. Prostate-specific membrane antigen expression as a predictor of prostate cancer progression. Hum Pathol. 2007; 38:696. [PubMed: 17320151]
14. Wright GL, Grob BM, Haley C, et al. Upregulation of prostate-specific membrane antigen after androgen-deprivation therapy. Urology. 1996; 48:326. [PubMed: 8753752]
15. Ross JS, Sheehan CE, Fisher HA, et al. Correlation of primary tumor prostate-specific membrane antigen expression with disease recurrence in prostate cancer. Clin Cancer Res. 2003; 9:6357. [PubMed: 14695135]
16. Minner S, Wittmer C, Graefen M, et al. High level PSMA expression is associated with early PSA recurrence in surgically treated prostate cancer. Prostate. 2011; 71:281. [PubMed: 20809553]
17. Liu H, Moy P, Kim S, et al. Monoclonal antibodies to the extracellular domain of prostate-specific membrane antigen also react with tumor vascular endothelium. Cancer Res. 1997; 57:3629. [PubMed: 9288760]
18. Bander NH, Trabulsi EJ, Kostakoglu L, et al. Targeting metastatic prostate cancer with radiolabeled monoclonal antibody J591 to the extracellular domain of prostate specific membrane antigen. J Urol. 2003; 170:1717. [PubMed: 14532761]
19. Milowsky MI, Nanus DM, Kostakoglu L, et al. Phase I trial of yttrium-90-labeled anti-prostate-specific membrane antigen monoclonal antibody J591 for androgen-independent prostate cancer. J Clin Oncol. 2004; 22:2522. [PubMed: 15173215]

20. Bander NH, Milowsky MI, Nanus DM, et al. Phase I trial of 177lutetium-labeled J591, a monoclonal antibody to prostate-specific membrane antigen, in patients with androgen-independent prostate cancer. J Clin Oncol. 2005; 23:4591. [PubMed: 15837970]

21. Tagawa ST, Milowsky MI, Morris MJ, et al. Phase II study of lutetium-177 labeled anti-prostate-specific membrane antigen (PSMA) monoclonal antibody J591 for metastatic castration-resistant prostate cancer. Clin Cancer Res. 2013; 19:5182. [PubMed: 23714732]

22. Tagawa ST, Vallabhajosula S, Osborne J, et al. Phase I trial of fractionated-dose ^{177}lutetium radiolabeled anti-prostate-specific membrane antigen (PSMA) monoclonal antibody J591 (^{177}Lu-J591) in patients (pts) with metastatic castration-resistant prostate cancer (metCRPC). J Clin Oncol, suppl. 2010; 28:7s.

23. Crook J, Robertson S, Collin G, et al. Clinical relevance of trans-rectal ultrasound, biopsy, and serum prostate-specific antigen following external beam radiotherapy for carcinoma of the prostate. Int J Radiat Oncol Biol Phys. 1993; 27:31. [PubMed: 7690016]

24. Pandit-Taskar N, O'Donoghue J, Beylergil V, et al. ^{89}Zr J591 immunoPET imaging in patients with prostate cancer (abstr 287). J Nucl Med. 2013; 54:287.

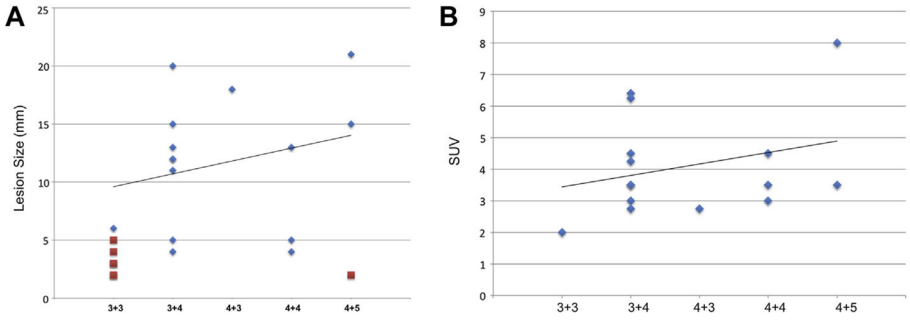

Figure 1.

A, correlation of Gleason score and lesion size with ex vivo PET detection of 11 index and 11 secondary lesions identified on histopathology. Diamonds indicate positive on microPET. Squares indicate negative on microPET. *B*, visible lesion SUV on ex vivo PET as function of Gleason score.

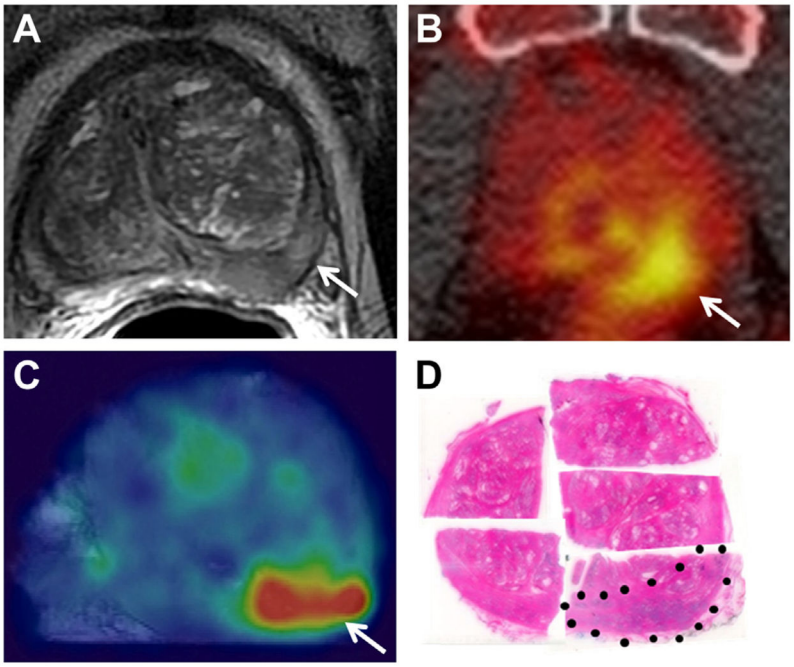

Figure 2.

Gleason 4 + 5 PCa in left posterior-mid peripheral zone. *A*, T2-weighted MRI. Arrow indicates cancer focus. *B*, in vivo PET. Arrow indicates cancer focus. *C*, ex vivo PET. Arrow indicates cancer focus. *D*, histopathology section. Dotted area indicates cancer. Reduced from ×1.

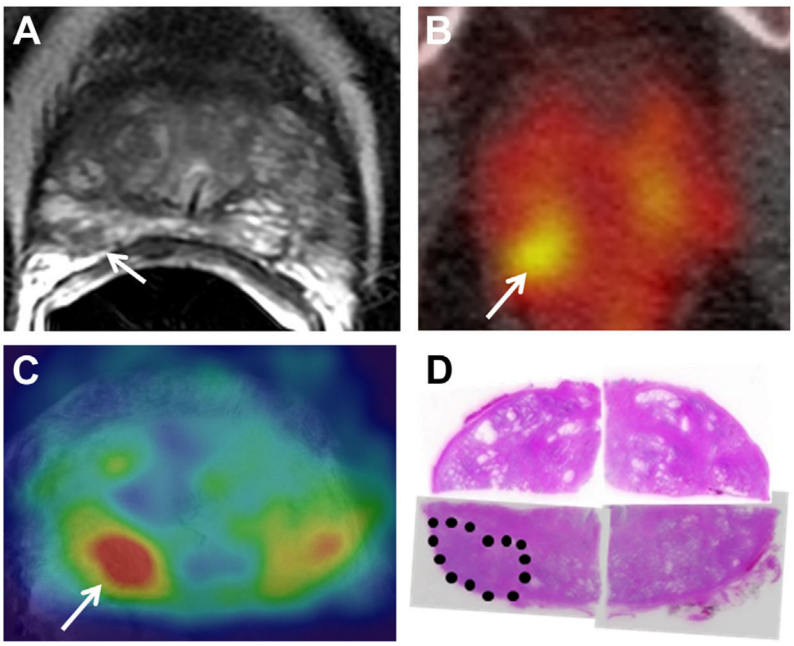

Figure 3.

Gleason 3 + 4 PCa in right posterior peripheral zone measured 9 mm. *A*, T2-weighted MRI showed limited restricted diffusion and limited enhancement, suggesting low suspicion for PCa. Arrow indicates cancer focus. *B*, in vivo PET. PET avidity suggested PCa. Arrow indicates cancer focus. *C*, ex vivo PET. PET avidity suggested PCa. Arrow indicates cancer focus. *D*, histopathology confirmed PCa (dotted area). Reduced from ×1.

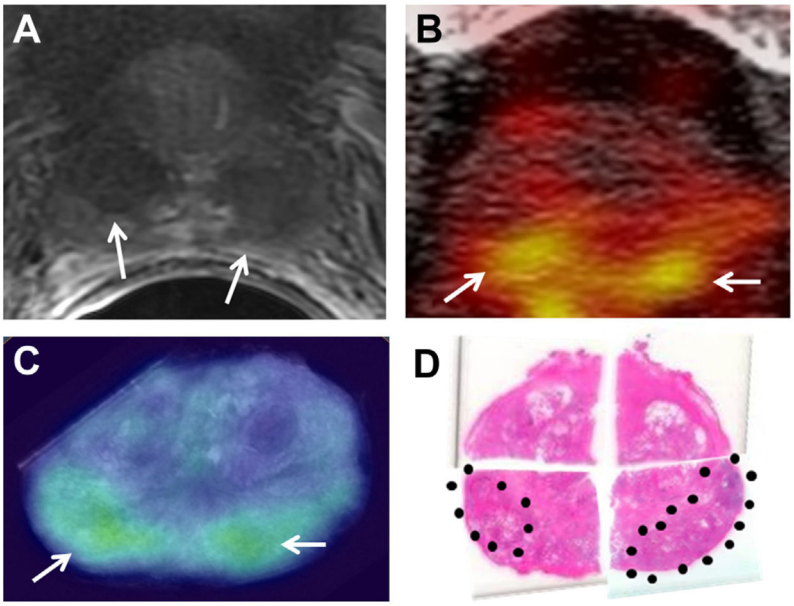

Figure 4.

Bilateral foci in posterior peripheral zone with Gleason score 3 + 4 at right and 4 + 3 at left. *A*, T2-weighted MRI. Arrows indicate foci. *B*, in vivo PET. Arrows indicate foci. *C*, ex vivo PET. Arrows indicate foci. *D*, histopathology section. Dotted areas indicate foci. Reduced from ×1.

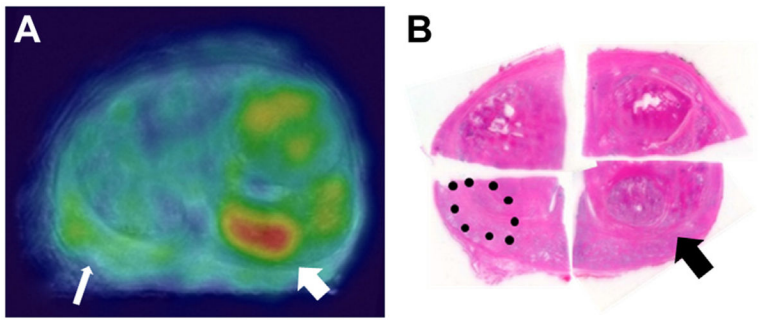

Figure 5.

Benign hyperplastic nodule (thick arrow) and Gleason 4 + 4 PCa (thin arrow). *A*, ex vivo PET. *B*, histopathology section. Reduced from ×1.

Table 1

Baseline characteristics

Pt—Age No.	Biopsy Gleason Score	PSA (ng/ ml)
1—62	3 + 4	3.5
2—62	3 + 4	4.8
3—68	4 + 5	12
4—54	4 + 3	4.8
5—63	4 + 3	5.2
6—47	3 + 4	4.8
7—63	3 + 4	6.5
8—61	3 + 4	5.4
9—58	4 + 3	6.5
10—58	3 + 4	4.8
11—60	4 + 5	11

Table 2

Radiological to pathological correlation

Lesion	Lesion Size (mm)	Final Pathology Gleason Score	Visible		MicroPET Uptake (SUV)
			In Vivo PET	Ex Vivo MicroPET	
Pt No. 1:					
Index	13	3 + 4	Yes	Yes	6.4
Secondary	2	3 + 3	No	No	–
Pt No. 2 (index)	12	3 + 4	Yes	Yes	3.5
Pt No. 3:					
Index	15	4 + 5	Yes	Yes	8
Secondary	5	3 + 3	No	No	–
Pt No. 4:					
Index	4	4 + 4	No	Yes	3
Secondary	3	3 + 3	No	No	–
Secondary	3	3 + 3	No	No	–
Pt No. 5:					
Index	5	4 + 4	No	Yes	3.5
Secondary	4	3 + 4	No	Yes	3.5
Pt No. 6:					
Index	11	3 + 4	Yes	Yes	3
Secondary	6	3 + 3	No	Yes	2
Pt No. 7:					
Index	20	3 + 4	Yes	Yes	6.25
Secondary	2	3 + 3	No	No	–
Pt No. 8:					
Index	18	4 + 3	Yes	Yes	2.75
Secondary	12	3 + 4	Yes	Yes	2.75
Pt No. 9 (index)	15	3 + 4	Yes	Yes	4.5
Pt No. 10:					
Index	13	4 + 4	No	Yes	4.5
Secondary	4	3 + 3	No	No	–

Lesion	Lesion Size (mm)	Final Pathology Gleason Score	Visible		MicroPET Uptake (SUV)
			In Vivo PET	Ex Vivo MicroPET	
Secondary	5	3 + 4	No	Yes	4.25
Pt No. 11:					
Index	21	4 + 5	Yes	Yes	3.5
Secondary	2	4 + 5	No	No	–

J Urol. Author manuscript; available in PMC 2015 April 28.